Design and experiment of air-suction roller corn precision dibbler based on DEM-CFD coupling

Yong Chen[1], Junwu He[1], Xing Yu[2], Bin Hu[3], Lianhao Li[1*], Xiuli Zhang[1], Xiaochan Liu[1], Ruonan Mao[1]

(1. *College of Mechanical and Electrical Engineering, Henan Agricultural University, Zhengzhou 450002, China*;
2. *Yellow River Institute of Hydraulic Research, Yellow River Conservancy Commission, Zhengzhou 450003, China*;
3. *College of Mechanical and Electronic Engineering, Shihezi University, Shihezi 832000, China*)

Abstract: Addressing the issues of poor performance and low single-seed rate during seed filling and cleaning for corn, an air-suction roller precision dibbler was designed, and its main structure and working principle were elaborated. Based on the structure of the seed metering disk and the tri-axial dimensions of corn seeds, an auxiliary filling type hole boss was designed with a radius of 4 mm and a thickness of 1.5 mm. A sawtooth-type seed cleaning device was also designed, with an installation angle greater than 3° and a serrated chamfer less than 62.1°. By coupling the Discrete Element Method (EDEM) with Computational Fluid Dynamics (CFD), the flow field structure and seed metering performance were simulated and analyzed, examining the movement states of the seed population and individual seeds during the processes of filling, cleaning, carrying, and initial seed dropping. The variation patterns of the internal flow field pressure and fluid velocity of the seed metering device under different negative pressures and operating speeds were studied. Through the construction of a test bench and single-factor and three-factor orthogonal experiments, along with multi-objective optimization methods, the primary and secondary factors affecting the qualification index were determined. The optimization results showed that when the flow field negative pressure was 3.52 kPa, the operating speed was 5.81 km/h, and the suction hole diameter was 4.15 mm, the qualification index of the seed metering device was 93.2%, the missed seeding index was 3.3%, and the multiple seeding index was 3.5%. An adaptability test was conducted to verify these results, revealing that the qualification index for all three varieties of corn seeds exceeded 92.4%, the missed seeding index was less than 3.7%, and the multiple seeding index was less than 3.9%, satisfying the precision seeding requirements for corn seeds.

Keywords: corn, air-suction roller precision dibbler, sawtooth seed cleaning, DEM-CFD coupling, orthogonal test
DOI: 10.25165/j.ijabe.20251805.9326

Citation: Chen Y, He J W, Yu X, Hu B, Li L H, Zhang X L, et al. Design and experiment of air-suction roller corn precision dibbler based on DEM-CFD coupling. Int J Agric & Biol Eng, 2025; 18(5): 142–153.

1 Introduction

Corn is the largest food crop in China, with its total output increasing year by year[1]. Single precision sowing is a new way to improve the economic coefficient under the condition of stable total biomass[2-4]. The core component of precision seeding technology is the seed metering device[5], and the pneumatic seed metering device, as the key to high-speed precision seeding technology, has been widely studied and applied in the field of seeding[6-8]. The air-suction seed-metering device adsorbs the seeds through the suction hole by relying on the air pressure difference inside and outside the negative pressure chamber. The distribution characteristics of the internal flow field of the seed-metering device are the key factors affecting its seeding performance[9,10].

In recent years, with the development of discrete element method (EDEM) and computational fluid dynamics (CFD), DEM-CFD gas-solid two-phase flow coupling simulation technology has been widely used in the field of agriculture[11-15]. Lai et al.[16] studied the influence of spring tension and other factors on the working performance of the chain spoon turnover precision metering device by using DEM and multibody dynamics (MBD) coupling method and verified the feasibility of the metering device by seeding adaptability test. Wang et al.[17] designed a kind of air-suction double-row staggered corn precision metering device and analyzed the working performance by DEM-CFD coupling method. Through bench and field experiments, it was concluded that the seeding qualification index was greater than 88.7% under the condition of operating speed of 5-10 km/h. Hu et al.[18] designed an internally pneumatic high-speed precision cotton seed metering device that utilizes double seed filling and secondary seed dropping methods to complete the seed planting process. The experimental results showed that the working performance of the seed metering device met the requirements for precision direct seeding of cotton. Aiming at the problems of low precision and poor uniformity of the traditional wheat seed metering device, Hou et al.[19] developed a wheat precision seed metering device with air suction filling and centrifugal cleaning. The performance of the seed metering device was studied and analyzed by combining theory with gas-solid

Received date: 2024-08-30 **Accepted date:** 2025-06-23
Biographies: **Yong Chen**, PhD, Associate Professor, research interest: agricultural machinery, Email: chenyong@henau.edu.cn; **Junwu He**, MS candidate, research interest: agricultural mechanization, Email: 15623803652@163.com; **Xing Yu**, PhD, Engineer, research interest: agricultural water-soil engineering, Email: yuxing1227@163.com; **Bin Hu**, PhD, Professor, research interest: mechanical design theory, Email: hb_mac@shzu.edu.cn.cn; **Xiuli Zhang**, PhD, Professor, research interest: agricultural equipment design, Email: zhangxiuli619@126.com; **Xiaochan Liu**, PhD, Lecturer, research interest: agricultural mechanization, Email: liuxiaochan@henau.edu.cn; **Ruonan Mao**, MS candidate, research interest: mechanization design, Email: 15713911335@163.com.

***Corresponding author: Lianhao Li**, PhD, Associate Professor, research interest: agricultural water-soil engineering. College of Mechanical and Electrical Engineering, Henan Agricultural University, Zhengzhou 450002, China. Tel: +86-13783608652, Email: lianhao8002@126.com.

coupling virtual simulation analysis (DEM-CFD). Pareek et al.[20] developed an air-blowing seed metering device to solve the problem of low success rate of seeding small-sized seeds with disc vacuum seed metering device. The experimental results showed that the seed metering device optimized the filling performance and improved the efficiency and accuracy of seeding operations. Sun et al.[21] designed an air-suction wheel-type seed-metering device incorporating an elastic pad to enhance seed extraction performance and analyzed velocity distributions across six different suction hole diameters to determine the optimal parameter range with FLUENT software. Jia et al.[22] developed an agitated seed metering device with horizontal seed filling and used DEM-CFD simulations to determine the optimal agitating plate angle by analyzing seed population migration patterns. Feng et al.[23] developed a high performance pneumatic seed metering device for carrot seeds and optimized the seeding plate hole geometry using FLUENT simulations, ultimately determining the optimal conical hole structure.

In conclusion, while previous research had concentrated on pneumatic and mechanical seed metering devices, their limitations in seed filling efficiency and high-speed precision seeding remain unresolved. This study therefore proposed an improved air-suction roller corn precision dibbler. It used the type hole bosses and the serrated seed clearing device to assist the seed filling. The DEM-CFD gas-solid coupling simulation technology was used to explore the filling mechanism of the drum-type dibbler, simulate the filling and initial seed dropping process, and optimize the structural parameters and working parameters of the metering device to improve the working performance of the drum-type dibbler. The working performance of the seed metering device was verified by bench test. The experimental results demonstrate that under optimal operating conditions—a flow field pressure of 3.52 kPa, an operating speed of 5.81 km/h, and a suction hole diameter of 4.15 mm—the dibbler achieves the seeding qualification index exceeding 92.4%, the seeding leakage index below 3.7%, and the seeding replay index under 3.9% across all three tested maize varieties. These performance metrics confirm the sowing adaptability and compliance with precision seeding requirements for corn.

2 Structure and working principle of seed metering device

The structure of the air-suction roller corn precision dibbler is shown in Figure 1. The hollow shaft body of the seed metering device is connected to the rear end cover of the seed metering device through a positioning bearing. The round flange-type bearing block is fixed by an interference fit with the shaft body through an internal bearing sleeve. The seed metering disk is fixed to the round flange bearing block with screws and forms a sealed vacuum negative pressure cavity with the inner chamber of the rear end cover of the seed metering device. The seed distribution disk is fixed to the wall of the rear end cover chamber with screws, and at the same time, the seed distribution teeth press tightly against the seed metering disk, serving as a fastening mechanism. After the seed metering ring is fixed to the belt, it is installed between the rear end cover and the cover plate of the seed metering device and secured with bolts. The front end cover of the seed metering device is connected to the shaft body through a flat key.

As shown in Figure 2, the seed metering device in this paper can be divided into five operational processes, namely, auxiliary seed filling, touch-based seed clearing, single-seed carrying, gas breaking and seed dropping, and secondary seed dropping. The

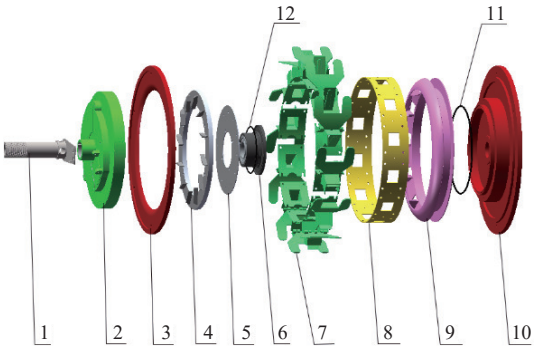

Note: 1. Hollow shaft body; 2. Front end cover; 3. Cover plate; 4. Seed distribution disk; 5. Seed metering disk; 6. Round flange-type bearing block; 7. Duckbill hole-forming device; 8. Belt; 9. Seed metering ring; 10. Rear end cover; 11. Rear end cover sealing ring; 12. Bearing block sealing ring.

Figure 1 Structural diagram of air-suction roller corn precision dibbler

secondary seed dropping is the process of depositing the seed into the soil by the duckbill hole-forming device. Under the action of the fan, the air pressure difference between the inside and outside sides of the seed metering disk is generated. Under the combined action of the suction holes and the type hole bosses on the seed metering disk, the corn seeds are separated from the population and adsorbed onto the suction holes of the seed metering disk. In the seed clearing area, the serrated seed clearing device on the front end cover of the seed metering device comes into contact with the seeds to perform the touch-based seed clearing operation, ensuring that only a single seed remains on each suction hole. In the seed dropping area, the action of the air cutoff valve block causes the pressure difference at the suction holes to disappear, allowing the seeds to fall onto the seed distribution disk and along the seed distribution teeth into the corresponding cavity of the seed metering ring, completing the initial seed dropping. At this time, the corn seeds in the cavity of the seed-metering ring slide down along the inner wall of the seed-metering ring into the duckbill hole-forming device to wait for the secondary seed dropping. When the duckbill hole-forming device is transferred to the seed-dropping position and contacts with the soil, the moving duckbill is pressed open, and the static duckbill completes the film-breaking hole-forming operation. At that moment, the seed falls into the soil hole along the inner wall of the static duckbill to complete the second seed-dropping.

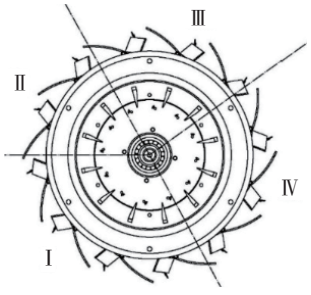

Note: I. Seed filling area; II. Seed cleaning area; III. Seed carrying area; IV. Seed dropping area

Figure 2 Division of working areas of seed metering device

3 Key structure design of seed metering device

3.1 Design of the seed metering disk structure

Before structural design, the tri-axis dimensions of three types of corn seeds - Xianyu 335, Zhengdan 958, and Jingke 968 - were

measured and analyzed. The seed dimensions were classified with a 1 mm interval, and the distribution of their tri-axial dimensions is shown in Figure 3. As can be seen from the frequency distribution graph, the length and width morphological characteristic parameters of the three types of corn seeds approximately follow a normal distribution. The lengths of the seeds are all distributed between 10 mm and 14.5 mm; the widths are all distributed between 7 mm and 10 mm; and the thicknesses are all distributed between 4.5 mm and 8 mm. There is no significant difference in the tri-axial dimension distribution.

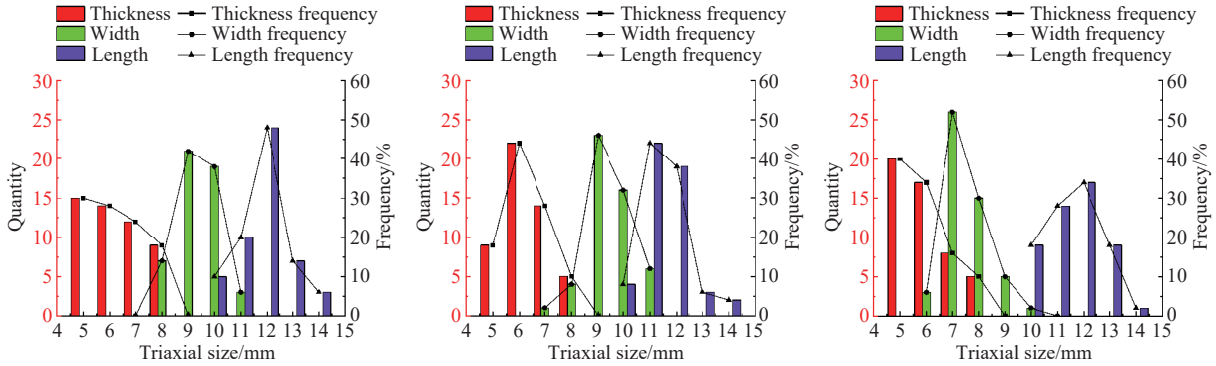

a. Xianyu 335 corn seeds b. Zhengdan 958 corn seeds c. Jingke 968 corn seeds

Figure 3 Frequency distribution of tri-axial dimensions of corn seeds

The role of the seed metering disk is to disturb the seed population and separate the seeds from it, as shown in Figure 4. The most important design parameters are the radius of the seed metering disk (R_1) and the number of seed suction holes (N). The diameter of the seed metering disk has a direct impact on the dimensions of the internal components of the seed metering device. After consulting relevant materials, it is known that there is a relationship between R_1 and N as shown below:

$$N \le \frac{2\pi R_1 v_m}{k v_x (1-\delta)} \tag{1}$$

where, N is the number of seed suction holes; R_1 is the radius of the seed metering disk, mm; v_m is the unit forward speed, m/s; k is the distance between hills, m; v_x is the linear velocity of the circle around the hole, m/s; δ is the walking slip rate of seeder.

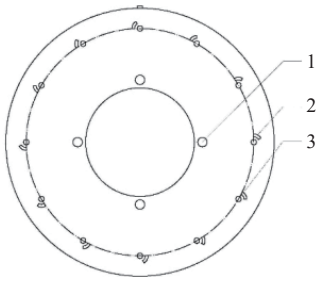

1. Positioning hole of the seed metering disk; 2. Type hole boss; 3. Suction hole

Figure 4 Seed dispenser of suction hole type seed metering device

The speed of seeding operation and the circumferential line speed of the suction hole of the seed metering device can be shown as follows:

$$\begin{cases} v_p = \dfrac{n_p}{60} N k \\ v_x = \dfrac{2\pi R_1 n_p}{k R_2 n_p} \end{cases} \tag{2}$$

where, v_p is the operating speed of seed metering device, m/s; n_p is the rotational speed of seed metering disk, r/min; R_2 is the radius of the center of the suction hole, mm.

By combining Equations (1) and (2), it can be obtained that:

$$\frac{v_p}{v_x} \ge \frac{kN}{2\pi R_2} \tag{3}$$

According to the agricultural machinery design manual, in this design, the diameter of the seed metering desk is set to 200 mm, the diameter range for the seed suction holes is 3-5 mm, and the radius to the center of the seed suction hole is 83.75 mm. Based on previous research results[24], the forward speed of the unit is less than or equal to 8 km/h, the rotation speed of the seed metering disk is less than or equal to 50 r/min, the walking slip rate is 10 %, and the plant spacing is set to 0.25 m. From these parameters, it can be calculated that the number of seed suction holes is 12.

3.2 Design of the type hole boss of seed metering disk

The structural characteristics of the seed metering disk are one of the key factors affecting the working performance of the seed metering device. The type hole boss is added outside the suction hole, and the main design parameters include the radius of the type hole boss (r') and the height of the type hole boss (h'). When designing the radius of the type hole boss (r'), the main consideration is to ensure the supporting force of the type hole boss on the seeds during the seed picking process. According to the measurement data of tri-axial dimensions of corn seeds, the average equivalent diameter of the three types of corn seeds is as follows:

$$\bar{D} = \frac{D_1 + D_2 + D_3}{3} \tag{4}$$

where, D_1, D_2, and D_3 are the equivalent diameter of Xianyu 335, Zhengdan 958, and Jingke 968, respectively. In order to ensure that the edge of the seed can contact with the type hole boss and ensure the support of the type hole boss to the corn seeds, the value of r' is half of $\bar{D}$.

$$r' = \frac{\bar{D}}{2} \tag{5}$$

According to calculation, the value of $\bar{D}$ is 7.99 mm, and the value of r' is 4 mm.

Selecting an appropriate height for the type hole boss (h') can effectively disturb the seed group, thereby enhancing the seed filling performance. In addition, after the seeds are adsorbed by the seed suction holes, as the seed metering disk rotates to the seed cleaning area, the supporting effect of the type hole boss on the seeds helps to reduce the energy consumption of the air-suction mechanical seed metering device, as shown in Figure 5.

During this process, the resultant force of the seed needs to satisfy Equation (6).

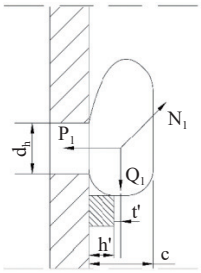

Figure 5 Stress analysis of the type hole boss

$$\begin{cases} P_1 \dfrac{d_h}{2} \geq Q_1 t' \\ P_1 = F_d = \dfrac{C_d \pi D^2 d_h^4 \Delta P}{256 r^4} \\ t' = c/2 - h' \end{cases} \tag{6}$$

where, F_d is the flow resistance of the seed in the flow field, N; P_1 is the resultant force in the horizontal direction, N; Q_1 is the resultant force in the vertical direction, N; ΔP is the pressure difference on both sides of the suction hole; c is the thickness of the seed, m; t' is the vertical distance from the center of mass of the seed to the surface of the type hole boss, m; r is the isotropic spherical radius, m; C_d is the coefficient of resistance to flow; d_h is the diameter of the seed suction hole, m; D is the equivalent diameter of the corn seed, m. From this, it can be concluded that the basic conditions that the seeds must meet in the process of moving with the seed metering disk to the seed cleaning area are the following equation:

$$\frac{C_d \pi D^2 d_h^5}{512 r^4} \Delta P \geq Q_1 \left(\frac{c}{2} - h' \right) \tag{7}$$

From Equation (7) , it can be seen that as the height of the type hole boss (h') increases, the pressure difference on both sides of the seed suction hole (ΔP) will decrease accordingly, thereby reducing energy consumption during the working process of the seed metering device. However, excessively high type hole bosses can lead to difficulties in seed cleaning, thereby increasing the rate of multiple seeding. Therefore, the value range of h' should ideally satisfy $0<h'<c/2$. Based on the measurement of tri-axial dimensions of corn seeds, the average thickness of corn seeds used in the test is 5.521 mm. In this design, the value of h' is selected to be 1.5 mm.

3.3 Design of the zigzag-shaped seed cleaning mechanism

The seed cleaning mechanism is an important part to ensure the single seed sowing of the seed metering device and is an important part of the precision seed metering device[25,26]. Currently, common seed cleaning mechanisms mainly include zigzag-shaped seed cleaning mechanism, brush-shaped seed cleaning mechanism, and elastic interspersed seed cleaning mechanism[27]. The zigzag-shaped seed cleaning mechanism is used to complete the seed cleaning operation in this study.

3.3.1 Installation position of the zigzag-shaped seed cleaning mechanism

The installation position of the seed cleaning mechanism should ensure that it can effectively remove excess seeds while also guaranteeing that the removed seeds can smoothly return to the seed population, avoiding blockage or scattering to other areas. The specific position analysis is shown in Figure 6. The installation position of the seed cleaning device is set as O_1 point, and the following equation can be obtained from Figure 6:

$$\begin{cases} Z_1 = R_2 \cos\phi \\ Z_2 = R_2 \cos\left(\phi + \dfrac{2\pi}{N}\right) \end{cases} \tag{8}$$

where, ϕ is the installation angle of the center position of the seed cleaning device relative to the horizontal plane, (°); Z_1 and Z_2 are the horizontal distances between the center of the seed suction hole and the center of the seed metering disk, respectively, mm.

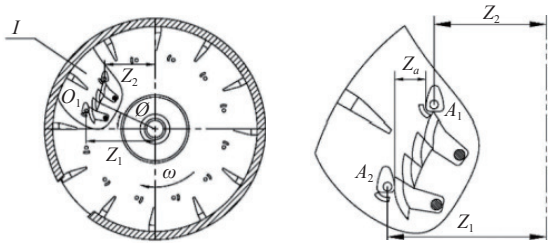

a. Overall schematic diagram b. Local enlarged view of Part I.

Figure 6 Analysis of the installation position of the zigzag-shaped seed cleaning mechanism

In order to avoid the collision between the cleaned seed and the adsorbed seed, the installation position must ensure that the distance between the two suction holes in the horizontal direction (Z_a) is greater than the maximum size of the corn seed. The maximum size of corn seeds used in the previous test was 13 mm. Therefore, the following equation should be satisfied when the seed cleaning device is installed:

$$Z_1 - Z_2 = R_2 \cos\phi - R_2 \cos\left(\phi + \frac{2\pi}{N}\right) > 13 \text{ mm} \tag{9}$$

After substituting the relevant data, it is found that: $\phi > 3°$.

3.3.2 Design of the chamfering of seed cleaning device

During the seed cleaning process of the seed metering device, the design of the serrated chamfer should allow the excess seeds at the seed suction hole to quickly slide off. The force condition is shown in Figure 7.

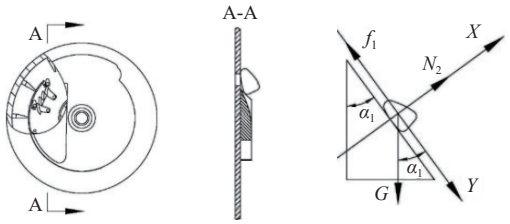

a. Overall schematic diagram b. A-A section c. Force analysis

Figure 7 Analysis of serrated chamfer

At the moment when the seed is being cleared and falls, it is subjected to its own gravity (G), as well as the influence of friction force (f_1) acting upward along the serrated surface and the supporting force (N_2) acting perpendicular upward to the serrated surface, as shown in Figure 7c. Here, the chamfer angle of the serrated seed clearing device edge is α_1, and the acceleration of seed is a_1.

The X-Y plane coordinate system is established with the seed centroid as the coordinate origin, and each force is projected onto the X-Y plane to obtain the following force balance equation:

$$\begin{cases} mg\cos\alpha_1 - f_1 = ma_1 \\ mg\sin\alpha_1 = N_2 \\ f_1 = \mu N_2 \end{cases} \tag{10}$$

According to Equation (10), it can be obtained that:

$$a_1 = g(\cos\alpha_1 - \mu\sin\alpha_1) \tag{11}$$

The cleared seeds will slide down along the edge angle of the

serrated seed cleaning mechanism. In order to avoid collision with the seeds near the seed suction hole, the falling distance Z_3 should be greater than the minimum size of 13 mm. Thus, Equation (12) can be obtained:

$$\begin{cases} Z_3 = \dfrac{1}{2}a_1 t^2 > 0.013 \\ t = \dfrac{2\pi R_2}{N v_p} \end{cases} \tag{12}$$

According to Equation (12), it can be obtained that:

$$Z_3 = \frac{1}{2}g(\cos\alpha_1 - \mu\sin\alpha_1)\left(\frac{2\pi R_2}{N v_p}\right)^2 > 0.013 \tag{13}$$

The static friction coefficient between corn seeds and organic glass plate is 0.459, and the maximum operating speed of the metering device is 14 km/h. The calculated α_1 is less than 62.1°.

4 Simulation modeling and analysis

The DEM-CFD coupling method was used to simulate and analyze the seeding operation process. This method realizes the interaction between the particle solid phase and the air fluid phase[28].

4.1 Simulation model establishment

In the case that the overall size of corn seeds is large and cannot meet the coupling calculation conditions, it is necessary to use the particle bonding replacement function of EDEM software to fill the corn seed model with smaller spherical particles, and use the Bonding model to bond several small ball particles together, so that a single small ball particle can be used as a part of the corn seed, and its volume fraction and power source phase can be calculated separately.

Firstly, the corn seeds were filled with small ball particles with a radius of 0.6 mm, and the coordinate information of the filled particles was derived[29]. The relevant parameter settings of EDEM software are listed in Table 1.

Table 1 Physical and mechanical property parameters required for simulation

Material	Poisson ratio	Shear modulus/Pa	Density/kg·m^{-3}
Corn seed	0.4	1.37×10^8	1.197
Seed plate material	0.5	1.77×10^8	1.18
Contact type	Restitution coefficient	Coefficient of static friction	Coefficient of kinetic friction
Seed-seed	0.182	0.431	0.0782
Seed-seed plate	0.621	0.459	0.0931

The tri-axial dimensional model of dibbler was established by Solidworks software and imported into EDEM, and the bonding replacement of corn seed simulation model particles was carried out by using the bonding model API program provided by the developer. The particle model required for the coupled virtual simulation is obtained, and the bonding results are shown in Figure 8.

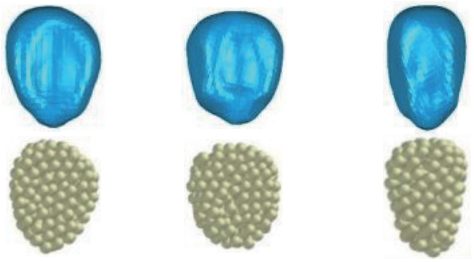

a. Large flat b. Circle-like c. Horse-tooth shape

Figure 8 Simulation model of corn seed

The seed metering device is simplified into four parts: front end cover, seed metering disk, seed distribution disk, and rear end cover. The solid phase model is established in EDEM, as shown in Figure 9. The fluid domain grid of the seed metering device is constructed by ICEM CFD, and the gas phase model is constructed by Fluent software, as shown in Figure 10.

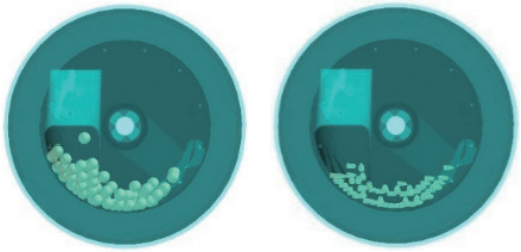

Figure 9 EDEM solid phase simulation model

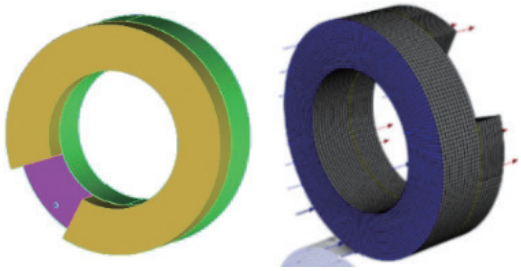

Figure 10 Fluent fluid phase simulation model

4.2 Analysis of seeding operation process

In the coupling simulation, the more particles involved in the simulation, the slower the calculation speed and the longer the calculation process. Therefore, under the premise of meeting the simulation requirements, the number of corn seeds involved in the simulation in this design is 60, and the total number of particles is about 20 000. Several simulation tests were carried out for different suction hole diameters, negative pressure of flow field, and rotation speed of seeding plate. It was found that when the diameter of seed suction hole was 4 mm, the rotation speed of seed metering disk was 4.19 rad/s, and the negative pressure of flow field was 3.5 kPa, the simulation effect was the best, and the qualification index of seeding operation was not less than 92.1%. The simulation process is shown in Figure 11.

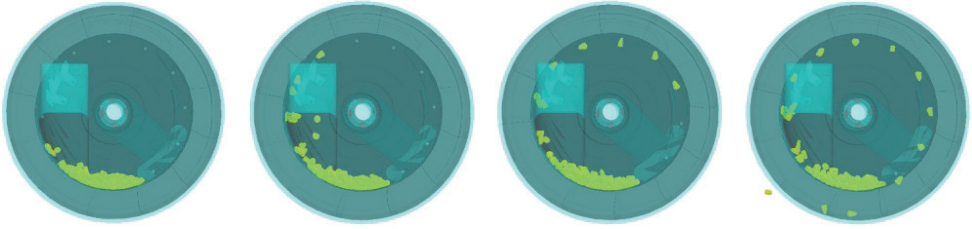

a. Seed filling process b. Seed cleaning process c. Seed carrying process d. Seed dropping process

Figure 11 Simulation process of seed metering device operation

The seed filling process, as shown in Figure 11a, involves the seed metering disk driving the seed population while the type hole boss on the seed metering disk perturbs the seed population, causing it to "boil" and enhancing the seed filling performance. This process results in seeds separating from the population and moving towards the seed cleaning area. The process of seed cleaning is shown in Figure 11b. After passing through the seed cleaning area, the multiple seeds that are adsorbed undergo the action of the serrated cleaning device, which retains only one seed to move with the suction hole to the seed carrying area. The seeds that are cleared fall back into the seed population under the influence of inertia and gravity, waiting for the next seed filling. The seed carrying process is shown in Figure 11c, where a single seed in this area moves at a uniform speed with the seed metering disk to the seed dropping area. After the corn seeds were transferred to the seed dropping area, the seeds were separated from the seed metering disk and entered the inner cavity of the seeding ring through the seed guide plate, as shown in Figure 11d. In addition, under the disturbance of the type hole boss, the flow performance of the population was significantly enhanced, and the seed filling efficiency was effectively improved.

4.3 Analysis of seed motion state in the process of seeding operation

In the process of seeding, the change of population velocity is shown in Figure 12.

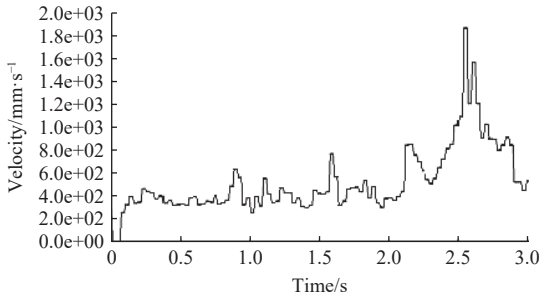

Figure 12 Diagram of speed changes during seed metering process

It can be seen from the diagram that in the process of filling, clearing, and carrying seeds, the overall speed of the population changes more evenly; in the process of 1.90-2.52 s, a single seed completed initial seed dropping and separated from the seed metering disk. During this period, due to the change of the motion state of the single seed, it changed from a uniform rotation motion with the seed metering disk to an irregular free fall motion. The rapid increase of the speed of the single seed caused the fluctuation of the overall speed of the population, and the peak speed appeared during the period of 2.53-2.61 s.

In order to further explore the movement state of single seed in the whole seeding process and study the change of seed movement speed, the simulation test of single seed is carried out under the condition that other conditions remain unchanged. In this process, the change of seed movement speed is shown in Figure 13.

It can be seen from Figure 13 that there are three reasons that affect the change of seed movement speed during the seeding process. The first is that the seed is captured by the suction hole, and the seed changes from a static state to a moving state. Secondly, in the process of seed cleaning, the serrated chamfer of the seed cleaning device collides with the seed, and the seed still moves with the seed plate under the condition of multiple forces. The third is that in the process of throwing seeds, the seeds are thrown once under the action of inertia force and gravity. During the period, the collision with the seed plate leads to a surge in speed, and finally the seeds are thrown once under the action of the seed plate. On the whole, the motion state of the seed is relatively stable during the whole seeding process.

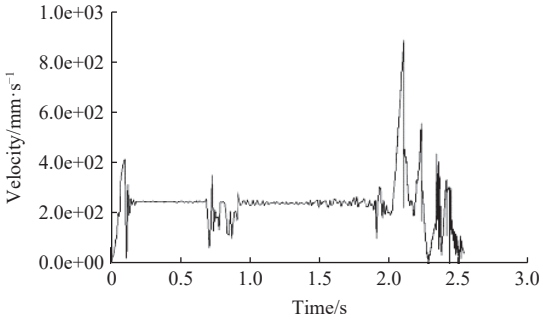

Figure 13 Motion state diagram of a single seed

4.4 The velocity change of the flow field inside the suction hole at different pressures

In order to further explore the influence of the change of air pressure on the internal flow field of the suction hole, the test and extraction of the speed of 40 r/min, a single suction hole in the air pressure of 2.0 kPa, 3.0 kPa, and 4.0 kPa flow field environment to complete a seeding cycle process, the specific value of the internal fluid velocity change, the integrated data as shown in Figure 14.

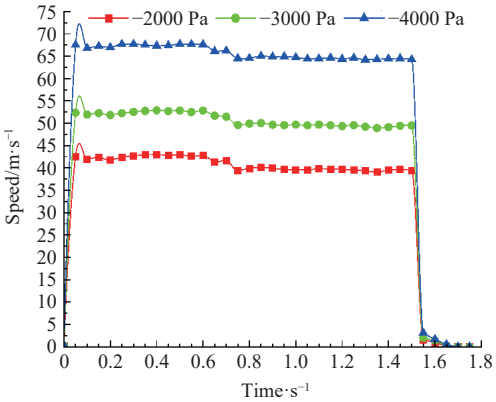

Figure 14 Velocity change of flow field in a single suction hole under different air pressures

As shown in Figure 14, the data storage interval during the coupling process was 0.05 s. After integration, 37 data points were retained and plotted for each pressure. In the process of 0.0-0.05 s, the coupling simulation began to instantly transfer the air pressure from the pressure outlet to the pressure inlet, and the pressure difference between the three fluid domains of the seed metering device was generated, which drove the air flow through the suction hole, and the velocity of the flow field in the hole was instantaneously increased. From 0.05 to 0.75 s, the process of seed filling and cleaning was carried out, and there was no great fluctuation in the flow field velocity inside the suction hole during this period. After 0.75 s, the excess seeds were cleaned backward by the seed cleaning device, leaving a single seed completely adsorbed on the suction hole, and the suction hole was in a blocked state, resulting in a decrease in the flow field velocity in the suction hole. During the period of 0.80-1.55 s, the seeds moved uniformly with the seed plate in the seed carrying area, and the velocity of the flow field in the hole was stable. Between 1.55-1.65 s, the seed moved to the seed throwing area, and the flow field in the suction hole was completely blocked by the air valve block, and the velocity of the

internal flow field decreased instantaneously. When it reached 1.80 s, the velocity of the flow field in the suction hole was almost 0 m/s. At this time, the seed fell from the seeding plate and fell to the cavity of the seeding ring after the seeding plate to complete a seeding process.

4.5 Change of flow field inside the suction hole at different rotational speeds

The rotation speed of the seed metering disc will affect the filling time, thus affecting the filling performance of the seed metering device. In this section, by changing the rotation speed of the seed plate, the change of the flow field of the seed metering device under the four rotation speeds of 20 r/min, 30 r/min, 40 r/min, and 50 r/min when the flow field pressure was 3.5 kPa in the coupling process was studied. Four rotational speeds were converted into angular velocities, and the angular velocities at four rotational speeds were 2.09 rad/s, 3.14 rad/s, 4.19 rad/s, and 5.24 rad/s, respectively. Figure 15 shows the pressure cloud diagram of the suction hole part after the same suction hole rotates 180° from the seed filling area to the seed carrying area at four different speeds.

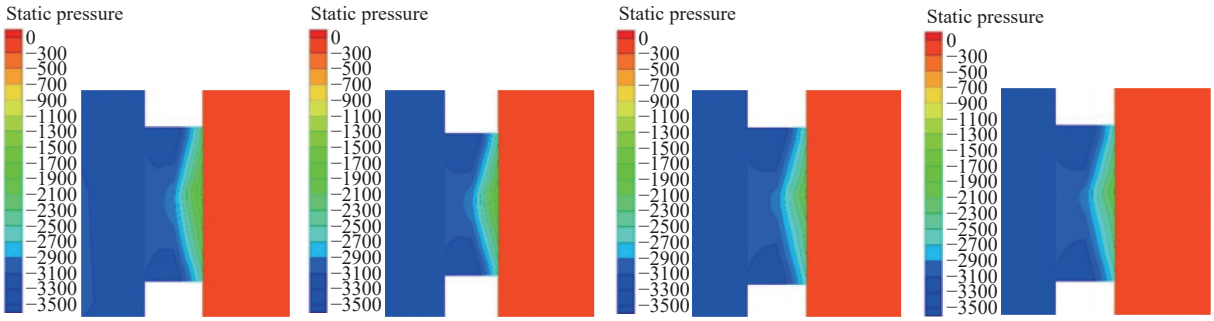

a. 20 r/min b. 30 r/min c. 40 r/min d. 50 r/min

Figure 15 Pressure contour maps of flow field under different rotational speeds

Comparing the pressure contours of the suction hole at four speeds in Figure 15, it could be seen that different speeds had little effect on the internal pressure distribution of the flow field. It could be seen from Figure 15 that the internal pressure of the suction hole was distributed in a banded superposition, and the pressure decreased step by step from the vacuum negative pressure chamber to the seed chamber, and with the increase of the rotational speed, the trend of this pressure decrease increased slightly.

In order to more intuitively show the influence of different rotational speeds on the flow field of the suction hole, the internal airflow velocity of the single suction hole under four rotational speeds was analyzed, and the internal airflow velocity distribution map of the vacuum negative pressure chamber and the single suction hole was obtained, as shown in Figure 16.

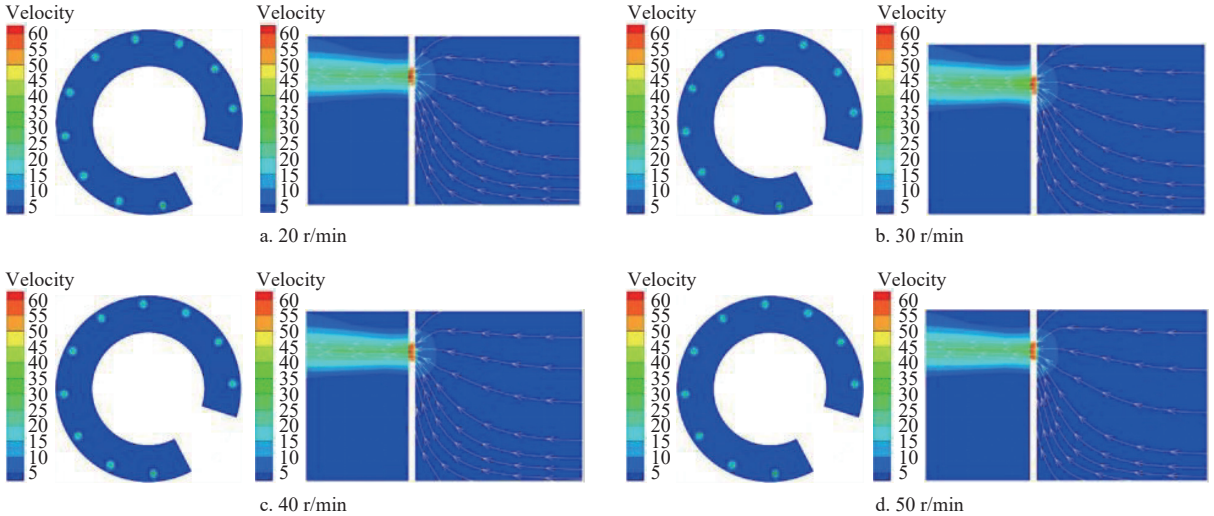

a. 20 r/min b. 30 r/min

c. 40 r/min d. 50 r/min

Figure 16 Velocity contour maps of flow field under different rotational speeds

As shown in Figure 16, Figures 16a-16d are the fluid velocity distribution contours inside the vacuum negative pressure chamber and a single suction hole when the rotation speed was 20 r/min, 30 r/min, 40 r/min, and 50 r/min, respectively. In Figure 16a, from left to right, the fluid velocity distribution cloud map inside the vacuum negative pressure chamber and the fluid velocity distribution cloud map inside the suction hole are respectively shown. It could be seen from the diagram that in the coupling process, the fluid velocity distribution in the three flow field areas inside the seed metering device was uniform. In the suction hole area, the fluid velocity was circularly distributed, and the fluid velocity increased gradually from the suction hole wall to the hole center. The maximum point of fluid velocity was located at the end of the suction hole near the pressure outlet of the flow field, and the maximum velocity could reach 55-60 m/s; the fluid velocity away from the suction hole area was below 5 m/s. The distribution of fluid velocity in Figures 16b-16d was almost the same as that in Figure 16a. The difference is that from Figures 16a-16d, the fluid velocity increased slightly from the periphery of the suction hole to the center of the hole, and this trend could be seen at the end of the

suction hole near the pressure outlet of the flow field. Comparing Figure 15, it could be seen that the change of fluid velocity and pressure conformed to mass conservation and Bernoulli's law.

5 Bench test

Through the previous theoretical calculation and simulation test analysis, the key structural parameters of the air-suction mechanical corn precision seed metering device were determined, and the prototype was modeled and manufactured by using three-dimensional software. The performance of the metering device needed to be combined with theoretical analysis and bench test for in-depth analysis, and the correctness of the theoretical calculation and simulation process was verified. In this experiment, the STB-700 seeding test bench was used to build the air-suction mechanical corn precision metering device. The motor speed, conveyor belt operating speed, and fan negative pressure could be adjusted on the console. In order to prevent the contact between the seed and the conveyor belt from beating during the seeding, a layer of hydraulic oil with uniform thickness was laid on the conveyor belt. The test bench is shown in Figure 17.

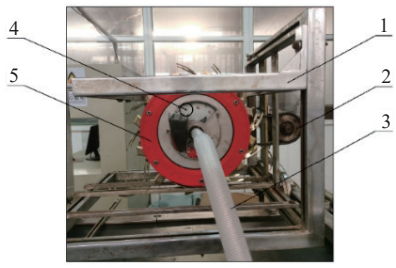

Note: 1. Seeding device fixing device; 2. Transmission system; 3. Negative pressure pipeline; 4. Single corn seed; 5. Air suction mechanical seed metering device

Figure 17 Bench test of seed metering device

5.1 Three-factor orthogonal test analysis

In order to explore the optimal performance parameter combination of seed metering device, it was necessary to carry out three-factor orthogonal test of flow field pressure, working speed, and suction hole diameter. According to the previous single-factor test results, it was found that when the flow field pressure was 3-4 kPa and the operating speed was 5-7 km/h, the seeding qualification index remained at a high level. The single-factor test results were summarized into a point-line diagram. The single-factor test results of operating speed and flow field pressure are shown in Figure 18 and Figure 19, respectively. According to the previous research on the characteristics of corn seed materials and the manual of agricultural machinery design, the suction hole diameter of the air-suction corn seed metering device should be less than 5.5 mm, so the diameter of the suction hole was determined to be 3-5 mm.

The advantages of multi-factor and multi-level experimental research are to enhance the design applicability, enhance the design excellence, and reduce the design capacity. It is a kind of experimental design method with high economic benefit and high efficiency [30].

The experimental design used Design-Expert 13 software and CCD experimental design method to design a three-factor quadratic orthogonal rotation combination test scheme. The factors and test level codes are listed in Table 2. According to the designed test scheme, the bench performance test was carried out. The test scheme and results are listed in Table 3.

The Design-Expert 13 software was used to fit and analyze the test results, and the quadratic polynomial regression model between the three response indices of the metering device and the three influencing factors was constructed. The regression equations are shown in Equations (14)-(16).

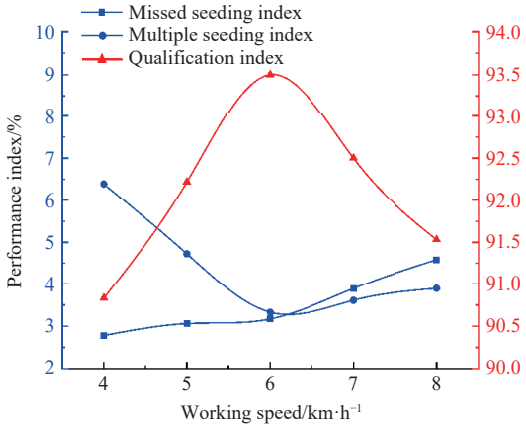

Figure 18 Single-factor test of operating speed for seed metering device

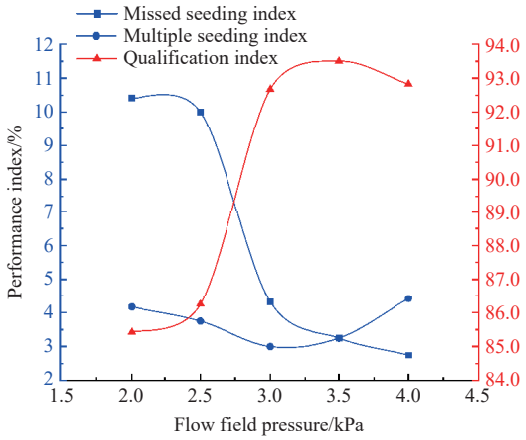

Figure 19 Single-factor test of flow field pressure for seed metering device

Table 2 Coding of factor levels in orthogonal experiment

Coding value	Flow field pressure A/-kPa	Operating speed B/km·h^{-1}	Suction hole diameter C/mm
Lower asterisk arm (–1.682)	2.66	4.32	2.32
–1	3	5	3
0	3.5	6	4
1	4	7	5
Upper asterisk arm (1.682)	4.34	7.68	5.68

$$M_1 = 93.81 + 0.54A + 0.51B - 2.23C - 0.14AB - 0.26AC + 0.14BC - 1.58A^2 - 1.17B^2 - 2.07C^2 \quad (14)$$

$$M_2 = 3.93 - 1.12A + 0.71B + 1.06C - 0.088AB - 0.49AC + 0.013BC + 0.93A^2 + 0.56B^2 + 0.77C^2 \quad (15)$$

$$M_3 = 2.27 + 0.58A - 1.22B + 1.17C - 0.23AB + 0.75AC - 0.15BC + 0.65A^2 + 0.61B^2 + 1.3C^2 \quad (16)$$

The test results were analyzed by variance analysis, and the analysis results are listed in Table 4.

Table 3 Orthogonal experimental scheme and results

Test	Impact factors			Corresponding indicators		
	Flow field pressure A/kPa	Operating speed B/ km·h^{-1}	Suction hole diameter C/mm	Qualification index M_1/%	Spread index M_2/%	Replay index M_3/%
1	–1	–1	–1	89.7	5.1	5.2
2	1	–1	–1	91.8	3.6	4.6
3	–1	1	–1	90.5	6.3	3.2
4	1	1	–1	92.9	5.7	1.4
5	–1	–1	1	84.9	7.6	7.5
6	1	–1	1	86.8	5.4	7.8
7	–1	1	1	87.1	10.1	2.8
8	1	1	1	87.6	6.3	6.1
9	–1.682	0	0	89.3	8.6	2.1
10	1.682	0	0	89.6	4.3	6.1
11	0	–1.682	0	90	4.5	5.5
12	0	1.682	0	91.2	6.3	2.5
13	0	0	–1.682	91.6	4.3	4.1
14	0	0	1.682	84.5	7.7	7.8
15	0	0	0	93.9	4.2	1.9
16	0	0	0	93.5	3.5	3
17	0	0	0	94.4	4.2	1.4
18	0	0	0	94.2	4.2	1.6
19	0	0	0	93.7	3.4	2.9
20	0	0	0	93.1	4.1	2.8

The variance analysis of the qualification index, missed seeding index, and multiple seeding index of the metering device was carried out. According to the prob<F test, that is, when the probability of $p>F$ is less than 0.05, the model is significant. It could be seen that the regression model of the three performance indices of the metering device was extremely significant, and the lack-of-fit term of the regression model was not significant, indicating that the fitting effect with the actual situation was good and there was no other main influencing factor affecting the response index. By testing the coefficients of the regression equation, the primary and secondary factors affecting the qualification index of seeding were as follows: flow field pressure, operating speed, suction hole diameter; the primary and secondary factors affecting the seeding leakage index were as follows: flow field pressure, operating speed, suction hole diameter; and the primary and secondary factors affecting the seeding replay index were as follows: operating speed, flow field pressure, suction hole diameter.

The three main influencing factors of the flow field pressure, operating speed, and suction hole diameter of the metering device were optimized. The seeding qualification index, missed seeding index, and multiple seeding index were used as the performance index function for optimization analysis. The mathematical model of nonlinear programming[31] was as follows:

$$\begin{cases} \text{target} \begin{cases} \max M_1 \\ \min M_2 \\ \min M_3 \end{cases} \\ \text{s.t.} \begin{cases} -4.34\ \text{kPa} < A < -2.66\ \text{kPa} \\ 4.32\ \text{km/h} < B < 7.68\ \text{km/h} \\ 2.32\ \text{mm} < C < 5.68\ \text{mm} \end{cases} \end{cases} \tag{17}$$

The Optimization-Numerical module in Design-Expert was used to optimize the solution, and the optimal operation combination parameters were obtained: the flow field pressure was 3.52 kPa, the operation speed was 5.81 km/h, and the suction hole diameter was 4.15 mm. The predicted value of the objective function was: the qualification index is 93.2%, the missed seeding index is 3.3%, and the multiple seeding index is 3.5%, which met the requirements of precision seeding of corn seeds.

Table 4 Variance analysis of multi-factor orthogonal experimental results and regression equations

Source of variance	Qualification index				Spread index				Replay index			
	Quadratic sum	DoF	F	p	Quadratic sum	DoF	F	p	Quadratic sum	DoF	F	p
Model	175.84	9	49.79	< 0.0001**	62.9	9	32.25	< 0.0001**	79.86	9	9.42	0.0008**
A	4.01	1	10.23	0.0095**	17.21	1	79.44	< 0.0001**	4.6	1	4.88	0.0006**
B	3.5	1	8.93	0.0136*	6.93	1	31.98	0.0002**	20.29	1	21.53	0.0009**
C	67.85	1	172.9	0.0221*	15.22	1	70.25	0.0101*	18.8	1	19.95	0.0012**
AB	0.1513	1	0.386	0.5486	0.0613	1	0.283	0.6066	0.405	1	0.429	0.5268
AC	0.5513	1	1.4	0.2633	1.9	1	8.77	0.0142*	4.5	1	4.78	0.0437*
BC	0.1513	1	0.386	0.5486	0.0013	1	0.006	0.941	0.18	1	0.191	0.6713
A^2	35.84	1	91.34	< 0.0001**	12.46	1	57.51	<0.0001**	6.04	1	6.41	0.0298*
B^2	19.74	1	50.31	< 0.0001**	4.5	1	20.76	0.001**	5.39	1	5.73	0.0378*
C^2	61.87	1	157.7	< 0.0001**	8.56	1	39.52	< 0.0001**	24.4	1	25.9	0.0005**
Residual error	3.92	10			2.17	10			9.42	10		
Lack of fit	2.8	5	2.5	0.1683	1.45	5	2.04	0.2267	6.87	5	2.69	0.1507
Error	1.12	5			0.7133	5			2.55	5		
Summation	179.77	19			65.06	19			89.29	19		

Note: ** Extremely significant ($p < 0.01$); * Significant ($p < 0.05$); and otherwise insignificant ($p > 0.05$).

5.2 Analysis of the effect of experimental factors

The response surface diagram was obtained by using Design-Expert 13 software and Origin software to process the experimental data, which can more intuitively analyze the relationship between each influencing factor and response index. Using the established regression model equation, one of the three influencing factors of flow field pressure, operating speed, and suction hole diameter was set to 3.5 kPa, 6 km/h, and 4 mm in turn, and the influence of the other two influencing factors and their interaction on the qualification index and leakage index of the seed metering device was analyzed. According to the regression equation of the qualification index of seeding, the response surface of each influencing factor to the qualification index and the missed seeding index of the seeding device is shown in Figures 20 and 21.

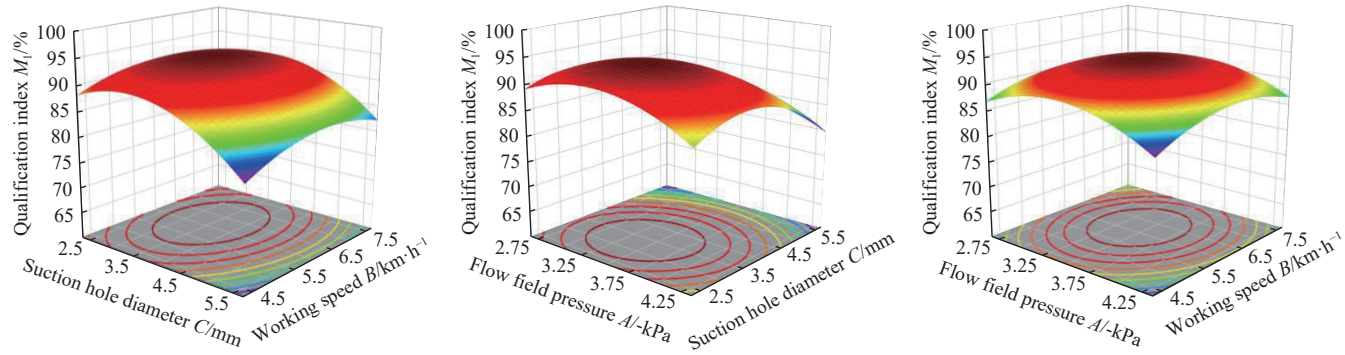

a. M_1 (3.5, B, C) b. M_1 (A, 6, C) c. M_1 (A, B, 4)

Figure 20 Response surface plot of qualification index of seed metering device

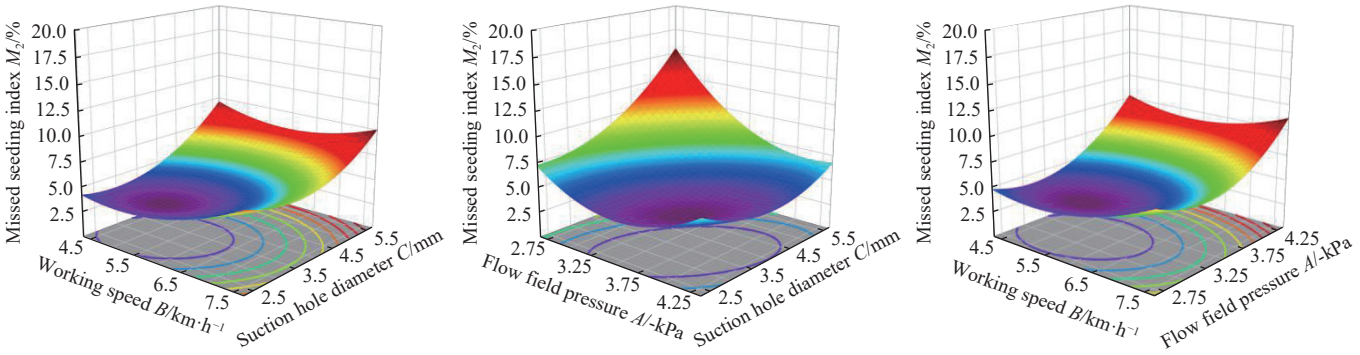

a. M_2 (3.5, B, C) b. M_2 (A, 6, C) c. M_2 (A, B, 4)

Figure 21 Response surface plot of missed seeding index of seed metering device

5.2.1 The influence of each influencing factor on the qualification index of seeding

Figure 20a is the influence of suction hole diameter and working speed on the qualification index of seeding when the flow field pressure was at the center level of 3.5 kPa. The analysis showed that with the increase of the operating speed of the metering device, the qualification index of seeding increased first and then decreased. The reason was that when the operating speed was greater than 6 km/h, due to the increase of the operating speed, the filling time was reduced, and the probability of the seed being adsorbed was reduced, resulting in an increase in the missed seeding index. With the increase of the diameter of the suction hole, the qualification index of seeding also showed a phenomenon of increasing first and then decreasing. The reason was that with the increase of the diameter of the suction hole, the adsorption force of the suction hole also increased, which improved the filling performance of the seed metering device, and the leakage index decreased. However, as the diameter of the suction hole continued to increase, multiple seeds would be adsorbed on the suction hole, the replay phenomenon was serious, and the replay index of seeding increased.

Figure 20b shows the influence of flow field pressure and suction hole diameter on the qualification index of seeding when the working speed was at the central level of 6 km/h. With the increase of flow field pressure, the qualification index of seeding increased first and then decreased. The reason was that when the flow field pressure was less than 3.5 kPa, with the increase of flow field pressure, the adsorption force at the suction hole gradually increased, which helped to improve the filling performance of the metering device. When the flow field pressure was greater than 3.5 kPa, as the flow field pressure continued to increase, the adsorption force of the suction hole continued to increase, and multiple seeds were adsorbed on the same suction hole, resulting in an increase in the multiple seeding index and a decrease in the qualification index. When the flow field pressure increased, the increase of the diameter of the suction hole would lead to a rapid increase in the adsorption force at the suction hole, resulting in a serious replay phenomenon, and resulting in a decrease in the qualification index of seeding. Similarly, when the flow field pressure was at a low level, the increase of the diameter of the suction hole would lead to a rapid decrease in the adsorption force at the suction hole, which would cause a serious leakage phenomenon, resulting in a decrease in the qualification index.

Figure 20c shows the influence of flow field pressure and working speed on the qualification index of seeding when the diameter of suction hole was 4 mm at the center level. With the increase of operating speed, the qualification index of seeding increased first and then decreased. The reason was that when the operating speed was low, the filling time was long and the clearing time was sufficient, which improved the filling performance of the metering device, thus improving the qualification index of seeding. When the operating speed was too large, the filling and clearing time of the metering device decreased, which would lead to the increase of the missed seeding index, thus reducing the qualification index of seeding. The qualification index of seeding increased first and then decreased with the change of flow field pressure. The reason was that under the premise of constant suction hole diameter, the increase of flow field pressure would lead to the gradual increase of adsorption force. If the adsorption force was too small, the missed seeding index would increase, and if the adsorption force was too large, the multiple seeding index would increase. Both of them would lead to the decrease of the qualification index of seeding.

5.2.2 The influence of each influencing factor on the missed seeding index

Figure 21a is the influence of suction hole diameter and

working speed on the qualification index of seeding when the flow field pressure was at the center level of 3.5 kPa. It could be seen from Figure 21 that under the condition that the flow field pressure was constant, with the increase of the operating speed of the metering device, the seeding leakage index gradually increased. The faster the operating speed was, the shorter the filling time was, and the lower the filling performance was, resulting in the continuous increase of the seeding leakage index. With the increase of the diameter of the suction hole, the seeding leakage index decreased first and then increased. The reason for this phenomenon was that when the flow field pressure was constant, the increase of the diameter of the suction hole within a certain range helped to improve the filling performance and reduce the seeding leakage index. At this time, the diameter of the suction hole continues to increase, resulting in a decrease in the adsorption force at the suction hole, which reduced the filling performance and caused the leakage index to rebound.

Figure 21b shows the influence of flow field pressure and suction hole diameter on the missed seeding index when the operating speed was at the central level of 6 km/h. It could be seen from the figure that when the operating speed remained unchanged, with the increase of the diameter of the suction hole and the pressure of the flow field, the index of seeding leakage decreased as a whole. The reason was that the increase of the diameter of the suction hole and the pressure of the flow field led to the increase of the adsorption force at the suction hole, which improved the filling performance and led to the increase of the multiple seeding index, resulting in the decrease of the index of seeding leakage.

Figure 21c shows the influence of flow field pressure and operating speed on the missed seeding index when the suction hole diameter was located at the central level of 4 mm. With the increase of the working speed of the metering device and the pressure of the flow field, the missed seeding index was on the rise as a whole. The reason was that the higher the speed of the metering device, the shorter the filling time of the seed plate, which reduced the filling performance and led to the phenomenon of missed sowing, resulting in the increase of the missed seeding index.

5.3 Experimental verification

Three types of corn seeds were used as test objects. Under the working conditions of flow field pressure of 3.52 kPa, operating speed of 5.81 km/h, and suction hole diameter of 4.15 mm, three sowing tests were repeated. The average value of the performance index results obtained from the test was taken. The test results are listed in Table 5.

Table 5 Test results of seed metering adaptability

Varieties	Response index		
	Qualification index/%	Spread index/%	Replay index/%
Xianyu 335	93.5	3.3	3.2
Zhengdan 958	93.1	3.3	3.6
Jingke 968	92.4	3.7	3.9

From Table 5, it could be seen that under the same working parameters, the seed metering device had certain adaptability to three different corn seeds. The test results showed that the seeding qualification index of the three corn seeds was greater than 92%, the seeding leakage index was less than 3.7%, and the seeding replay index was less than 3.9%, which met the requirements of corn seed precision seeding. Among them, Jingke 968 corn seeds were mostly horse-toothed, and their triaxial size distribution was quite different. The spherical rate was 65.5%. The fluidity was relatively poor during the seeding process, so the seeding performance index was relatively poor. The seeding effect of the Jingke 968 seeds is shown in Figure 22.

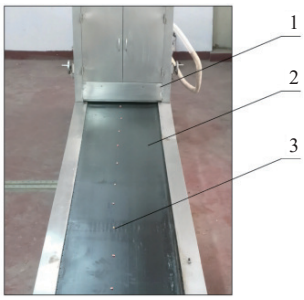

1. STB-700 seeding test bench; 2. Conveyor belt; 3. Corn seeds

Figure 22 Adaptability test effect diagram of Jingke 968 seed planting

6 Conclusions

1) The diameter of the seeding plate was determined to be 200 mm, and the number of suction holes and the number of type hole bosses were both 12. The type hole bosses and the serrated seed clearing device were designed to assist the seed filling, and the basic structural parameters were determined by force analysis.

2) The coupling virtual simulation test was used to analyze the variation law of the internal flow field pressure and fluid velocity of the seed metering device under different negative pressures and operating speeds. The filling, cleaning, carrying, and one-time throwing processes of the seeding operation were analyzed, and the movement state of the population and single seed during the seeding operation was analyzed. The simulation test found that when the negative pressure of the flow field was 3.5 kPa, the rotation speed of the seed plate was 4.19 rad/s, and the diameter of the suction hole was 4 mm, the qualification index of the metering device was higher than 92.1%.

3) Through single-factor and three-factor orthogonal tests and multi-objective optimization method, the primary and secondary factors affecting the qualification index of seeding were determined. Through the seeding adaptability bench test, it was found that when the flow field pressure was 3.52 kPa, the operating speed was 5.81 km/h, and the suction hole diameter was 4.15 mm, the seeding qualification index of the three varieties of corn seeds was greater than 92.4%, the seeding leakage index was less than 3.7%, and the seeding replay index was less than 3.9%. The seeding adaptability was good and met the requirements of corn seed precision seeding.

Acknowledgements

This work was supported by the Joint Fund for Science and Technology Research and Development Project of Henan Province of China (Grant No. 242103810026), the Outstanding Youth Project of Xinjiang Production and Construction Corps (Grant No. 2024DB002), and the Scientific and Technological Research Project in Henan Province (Grant No. 252102110357).

[References]

[1] Chen Y J, Wang Q Q, Xiang Y. Analysis on the status superiority and self-sufficiency ratio of maize in China. Chinese Journal of Agricultural Resources and Regional Planning, 2019; 40(1): 7–16.

[2] Xing H, Wang Z M, Luo X W, He S Y, Zang Y. Mechanism modeling and experimental analysis of seed throwing with rice pneumatic seed metering device with adjustable seeding rate. Computers and Electronics in

Agriculture, 2020; 178(5): 396–412.
[3] Zhang J L, Geng Y, Guo F, Li X G, Wan S B. Research progress on the mechanism of improving peanut yield by single-seed precision sowing. Journal of Integrative Agriculture, 2020; 19(8): 1919–1927.
[4] Han D D, Zhang D X, Jing H R, Yang L, Cui T, Ding Y Q, et al. DEM-CFD coupling simulation and optimization of an inside-filling air-blowing maize precision seed-metering device. Computers and Electronics in Agriculture, 2018; 150(5): 426–438.
[5] Yang L, Yan B X, Zhang D X, Zhang T L, Wang Y X, Cui T. Research progress on precision planting technology of maize. Transactions of the CSAM, 2016; 47(11): 38–48.
[6] Yang L, Shi S, Cui T, Zhang D X, Gao N N. Air-suction corn precision metering device with mechanical supporting plate to assist carrying seed. Transactions of the CSAM, 2012; 43(Z1): 48–53.
[7] Karayel D, Barut Z B, Özmerzi A. Mathematical modelling of vacuum pressure on a precision seeder. Biosystems Engineering, 2004; 87(4): 437–444.
[8] Yan B X, Zhang D X, Cui T, He Z T, Ding Y Q, Yang L. Design of pneumatic maize precision seed-metering device with synchronous rotating seed plate and vacuum chamber. Transactions of the CSAE, 2017; 33(23): 15–23.
[9] Yuan Y M, Ma X, Jin H X, Yin H Y. Study on vacuum chamber fluid field of air suction seed-metering device for rice bud-sowing. Transactions of the CSAM, 2005; 36(6): 42–45.
[10] Shi L R, Wu J M, Sun W, Zhang F W, Sun B G, Liu Q W, et al. Simulation test for metering process of horizontal disc precision metering device based on discrete element method. Transactions of the CSAE, 2014; 30(8): 40–48.
[11] Chen Y, Gao X X, Jin X, Ma X R, Hu B, Zhang X L. Calibration and analysis of seeding parameters of *Cyperus esculentus* seeds based on discrete element simulation. Transactions of the CSAM, 2023; 54(12): 58–69. DOI: 410.6041/j.issn.1000-1298.2023.12.005. (in Chinese)
[12] Shi S, Liu H, Wei G J, Zhou J L, Jian S C, Zhang R F. Optimization and experiment of pneumatic seed metering device with guided assistant filling based on EDEM-CFD. Transactions of the CSAM, 2020; 51(5): 54–66.
[13] Lai Q H, Jia G X, Su W, Zhao L J, Qiu X B, Lv Q. Design and test of chain-spoon type precision seed-metering device for ginseng based on DEM-MBD coupling. Transactions of the CSAM, 2022; 53(3): 91–104.
[14] Wang G W, Xia X M, Zhu Q H, Yu H Y, Huang D Y. Design and experiment of soybean high-speed precision vacuum seed metering with auxiliary filling structure based on DEM-CFD. Journal of Jilin University (Engineering and Technology Edition), 2022; 52(5): 1208–1221.
[15] Wang L J, Yu Y T, Zhang S, Song L L, Feng X. Motion characteristics of maize mixture on bionic screen based on earthworm motion characteristics. Transactions of the CSAM, 2022; 53(3): 158–166.
[16] Lai Q H, Xie G F, Su W, Zhao J W, Sun W Q, Chen Z Y. Design and experiment of precision seed metering device for broad bean with chain spoon flipping seed cleaning. Transactions of the CSAM, 2022; 53(8): 82–92. (in Chinese)
[17] Wang W W, Song L Z, Shi W B, Wei D H, Chen Y X, Chen L Q. Design and experiment of air-suction double-row staggered precision seed metering device for maize dense planting. Transactions of the CSAM, 2024; 55(3): 53–63.
[18] Hu M J, Xia J F, Zheng K, Du J, Liu Z Y, Zhou M K. Design and experiment of inside-filling pneumatic high speed precision seed-metering device for cotton. Transactions of the CSAM, 2021; 52(8): 73–85.
[19] Hou J L, Ma D X, Li H, Zhang Z L, Zhou J L, Shi S. Design and experiment of pneumatic centrifugal combined precision seed metering device for wheat. Transactions of the CSAM, 2023; 54(10): 35–45.
[20] Pareek C M, Tewari V K, Rajendra M. Multi-objective optimization of seeding performance of a pneumatic precision seed metering device using integrated ANN-MOPSO approach. Engineering Applications of Artificial Intelligence, 2023; 117: 105559.
[21] Sun Y H, Guo J H, Shi L R. Design and parameter optimization of air-suction wheel type of seed-metering device with elastic pad for maize. Int J Agric & Biol Eng, 2024; 17(4): 116–127.
[22] Jia H L, Chen Y L, Zhao J L, Guo M Z, Huang D Y, Zhuang J. Design and key parameter optimization of an agitated soybean seed metering device with horizontal seed filling. Int J Agric & Biol Eng, 2018; 11(2): 76–87.
[23] Feng D H, Sun X P, Li H, Qi X D, Wang Y J, Nyambura, S M. Optimized design of the pneumatic precision seed-metering device for carrots. Int J Agric & Biol Eng, 2023; 16(6): 134–147.
[24] Ren D L, Liu T, Xia S H, Chen Y X, Wang W W, Li Z D. Design and seed filling performance test of cavity plate combination hole type seeding plate for corn and soybean. Transactions of the CSAM, 2024; 55(2): 73–89.
[25] Chen H T, Li T H, Wang H F, Wang Y, Wang X. Design and parameter optimization of pneumatic cylinder ridge three-row close-planting seed-metering device for soybean. Transactions of the CSAE, 2018; 34(17): 16–24.
[26] Chen M Z, Diao P S, Zhang Y P, Gao Q M, Yang Z, Yao W Y. Design of pneumatic seed-metering device with single seed-metering plate for double-row in soybean narrow-row-dense-planting seeder. Transactions of the CSAE, 2018; 34(21): 8–16.
[27] Chen L D. Performance parameter design of air-suction seed metering device and experiment study of effects on sowing quality. MS dissertation. Heilongjiang: Heilongjiang Bayi Agricultural University, 2006; 8. 63p. (in Chinese)
[28] Ding W. Research on the particle-fluid two-phase coupling model based on CFD-DEM. MS dissertation. Shanghai: Shanghai Jiao Tong University, 2023; 2. 86p. (in Chinese)
[29] Ding L, Yang L, Zhang D X, Cui T, Li Y H, Gao X J. Design and test of unloading mechanism of air-suction seed metering device. Transactions of the CSAM, 2020; 51(1): 37–46.
[30] Sun S C. Simulation analysis of working process of air suction corn precision seed-metering device based on DEM-CFD coupling method. MS dissertation. Jilin: Jilin University, 2016; 9. 101p. (in Chinese)
[31] Zhao Z, Li Y M, Chen J, Zhou H. Dynamic analysis on seeds pick-up process for vacuum-cylinder seeder. Transactions of the CSAE, 2011; 27(7): 112–116.